www.czasopisma.pan.pl PAN www.journals.pan.pl
Chemical and Process Engineering 2019, 40 (2), 145–155
DOI: 10.24425/cpe.2019.126107

Cellular-automata based modeling of heterogeneous biofilm growth for microbiological processes with various kinetic models

Szymon Skoneczny*

Cracow University of Technology, Department of Chemical and Process Engineering,
ul. Warszawska 24, 30-155 Kraków, Poland

The study concerns modeling and simulation of the growth of biofilms with heterogeneous structures with a discrete mathematical model based on theory of cellular automata. The article presents two-dimensional density distributions of biofilms for microbial processes: oxidation of ammonium by *Nitrosomonas europaea* bacteria and glucose utilization by *Pseudomonas aeruginosa* bacteria. The influence of limiting substrate concentration in the liquid phase on biofilm structure was determined. It has been shown that the value of death rate coefficient of microorganisms has the qualitative and quantitative influence on the density and porosity of the biofilm.

Keywords: biofilm structure, cellular automata, mathematical modeling

1. INTRODUCTION

Biofilm is a multi-component layer formed on a solid substratum containing microbial cells and extracellular polymeric substances. Biofilm is a complex object, regarding its composition, morphology, and processes proceeding therein. Understanding the mechanism of biofilm formation and its functioning is necessary to improve the efficiency of technological processes carried out with its participation. Predicting the structure of the biofilm by means of mathematical models is a complicated issue because of numerous phenomena involved in its creation. These phenomena include among others: hydrodynamics (Duddu et al., 2009; Peyton, 1996), type of substratum (Flint et al., 2000) and substrate load (Peyton, 1996). This knowledge is crucial for issues related to the engineering of microbiological reactors. On the other hand, it is necessary to develop efficient methods of removing harmful biofilms.

Theoretical studies concerning morphology of biofilms were conducted with two- and three-dimensional discrete mathematical models, which are based on treating time and space in a quantified manner (Picioreanu et al., 1998b). In cellular automata and individual-based models, belonging to this group, a complex biofilm structure emerges as a result of interactions of the biomass units with each other and the environment (Kreft et al., 2001). Discrete models can be used for the determination of density and porosity distributions in the biofilm. Both quantities have a fundamental influence on the transport of substrates and rate of the processes occurring in the biofilm (Skoneczny, 2017).

In biotechnology both heterotrophic and autotrophic microorganisms are used. The first require presence of organic carbon for growth. These microorganisms are used, e.g. in the biodegradation of toxic carbonaceous

* Corresponding author, e-mail: skoneczny@chemia.pk.edu.pl

compounds such as phenol, dichlorophenol, toluene or benzene. In turn, autotrophs are used, e.g. for oxidation of ammonium to nitrite. This group includes *Nitrosomonas* and *Nitrobacter* bacteria. The rate of microbiological processes involving heterotrophic and autotrophic microorganisms is significantly different from each other.

Despite the proven influence of the rate of biofilm growth on its structure, there are no, as yet, studies aimed at identifying differences between structures of biofilms in which microbiological processes follow various kinetic models. This paper presents the results of simulations for two microbial processes: oxidation of ammonium by bacteria *Nitrosomonas europaea* and degradation of glucose by bacteria *Pseudomonas aeruginosa*. *Nitrosomonas europaea* are autotrophic bacteria, while *Pseudomonas aeruginosa* are heterotrophic bacteria. Kinetic equations for these processes are different.

2. MATHEMATICAL MODEL

The proposed mathematical model of biofilm growth (Skoneczny, 2013) is based on the cellular automata theory. It can be used for modeling of microbiological processes following single- and multi-substrate kinetics. The model allows for the partial processes such as diffusion and utilization of reactant, growth and death of microorganisms and biofilm detachment. In order to assess the influence of the kinetics of the microbiological process on the biofilm structure, simulations in this study did not take into account the detachment phenomenon. Otherwise, the resulting structure would be the result of the kinetics of microbiological process and detachment, which would make comparative assessment difficult.

Cellular automaton is a mathematic concept consisting of the following elements (Kułakowski, 2000):

- grid of cells $\{i\}$ of D-dimensional space;
- set $\{s_i\}$ of single cell's states;
- transition function F, i.e. a set of rules, determining the cell's state at moment $t + 1$ depending on the state of that cell and cells surrounding it, at moment t:

$$s_i(t+1) = F\left[\left(s_j(t)\right)\right], \quad j \in \Omega(i) \tag{1}$$

where $\Omega(i)$ is a neighborhood of i-th cell. In the 2-D rectangular grid, von Neumann or Moore neighborhood (Fig. 1) is most often used.

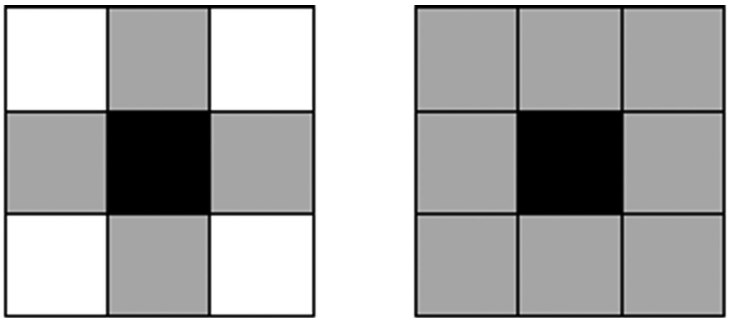

Fig. 1. von Neumann neighborhood (left) and Moore neighborhood (right); grey color denotes cells which are neighbors of the central cell

Two-dimensional overlaying grids with square cells have been used in this study. The substrate's grids contain information about the concentrations of the limiting substrate, while the biomass grid contains information about the presence and biological state of microorganisms.

Neighborhood proposed by von Neumann (Fig. 1) was used in the model. Periodic conditions were implemented on the borders of the grid. At the fixed distance from the front of the biofilm at each iteration, the state of cells was equal to c_i^c, i.e. concentration of the limiting substrate i in bulk liquid. The state of cells of the grid for the substrate can be a value in the range $\mu \in [0, c_i^c]$. For biomass, the values of μ belong to the set $\mu \in [0, \rho_b^{\max}]$.

Since the reaction and diffusion processes take place at a much higher rate than biofilm growth, it is assumed that the distribution of the limiting substrate concentration reaches pseudo-steady state. This results in distinguishing two time steps of significantly different values. Time step Δt, of the order of milliseconds is related to reaction and diffusion processes, while Δt_g time step, of the order of hours, refers to the processes of biomass growth and death. Time step Δt is related to grid element size by the following formula (Skoneczny, 2015):

$$\Delta t = \frac{(\Delta x)^2}{4D_w} \tag{2}$$

Rules governing the proposed cellular automaton are described below.

Rule 1 – diffusion of the substrate

Diffusion process was simulated in this study using the algorithm of random walks in a modified version. The probabilities of movement of the mass quantum of the limiting substrate i in the liquid phase in all four directions in the grid are the same and equal P_{dw}, and the sum of these probabilities is equal to one. Movement probability of the mass quantum depends on the presence of biomass in the starting and the target cell. It was calculated as follows:

$$P_d = P_w \cdot \left(\frac{n_w}{2} + \frac{D_b}{D_w} \frac{n_b}{2} \right) = 0.25 \cdot \left(\frac{n_w}{2} + \frac{D_b}{D_w} \frac{n_b}{2} \right) \tag{3}$$

The above equation is useful for both water and biofilm. In Eq. (3) n_b is the number characterizing the system of two cells: the starting and the target one. It specifies the sum of cells in this doublet, which represent the biomass. In turn, n_w is the number related to the presence of water in the same doublet of cells. Both n_b and n_w can take values from the set $\{0, 1, 2\}$.

Rule 2 – utilization of substrates in the biofilm

Using Eq. defining the substrate utilization rate, we have

$$r_i^b = -\frac{c_i^b}{dt} \approx -\frac{\Delta c_i^b}{\Delta t} \tag{4}$$

Based on the above relationship, the expression determining the increase in the substrate concentration during time step Δt can be obtained. This expression is shown below

$$\Delta c_i^b(k,l,t) = -\Delta t \cdot r_i^b \left[c_i^b(k,l,t), \rho_b(k,l,t) \right] \tag{5}$$

where k and l denote indexes of a cell in the grid for the limiting substrate.

Rule 3 – Growth and death of microorganisms

Change in the density of microorganisms during time step Δt_g is determined using Eq. (6):

$$\Delta \rho_b(k,l,t) = \Delta t_g \cdot r_{\mathrm{B}}^b \left[c_i^b(k,l,t), \rho_b(k,l,t) \right] - \Delta t \cdot r_o^b \left[\rho_b(k,l,t) \right] \tag{6}$$

The algorithm of biomass spreading according to Picioreanu et al. (1998a) was implemented in the model. This algorithm is described in Appendix A.

In order to quantitatively describe conditions of biofilm growth, so-called G group will be used. It is a dimensionless number proposed by Picioreanu et al. (1998b), defined as:

$$G = \frac{L_b^2 k \rho_b^{\max}}{D_{ei} c_i^c} \tag{7}$$

Symbol c_i in Eq. (7) denotes the concentration of a liming substrate. Picioreanu et al. (1998b) distinguish "transport limited regime" when G is high, and "growth-limited regime" when G takes low values.

The algorithm for the dynamical simulation of the biofilm growth is presented in Fig. 2.

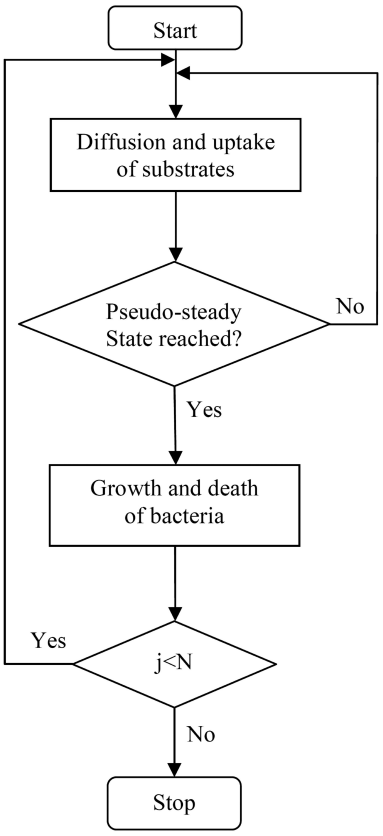

Fig. 2. Algorithm for dynamic simulation of biofilm growth with cellular-automata based model

3. RESULTS AND DISCUSSION

In order to simulate thin biofilm layer attached to the substratum at initial time $t = 0$, in the last row of the grid for biomass, the value of cells' state was set to $\mu = \rho_b^{\max}$, while the value of remaining cells' state was $\mu = 0$. Other simulation parameters are shown in Table 1.

Figure 3 shows the structure of the biofilm of nitrifying bacteria *Nitrosomonas europaea* in oxidation of ammonium. The kinetics of growth of these bacteria is described by Eqs. (8). These bacteria are autotrophic, with a relatively low value of the specific growth rate. Eqs. (8) are proposed by Wijffels et al. (1994).

$$r_{\mathrm{T}}^b \left(c_{\mathrm{T}}^b, \rho_b\right) = \left(\frac{k}{w_{\mathrm{BT}}} + m_{\mathrm{T}}\right) \frac{c_{\mathrm{T}}^b}{K_{\mathrm{T}} + c_{\mathrm{T}}^b} \rho_b \tag{8a}$$

$$r_{\mathrm{B}}^b \left(c_{\mathrm{T}}^b, \rho_b\right) = w_{\mathrm{BT}} \cdot \left(r_{\mathrm{T}} \left(c_{\mathrm{T}}^b, \rho_b\right) - m_{\mathrm{T}} \rho_b\right) \tag{8b}$$

Table 1. Values of parameters used in simulations

Parameter	Value	Dimension
c_{A}^{c}	2.62×10^{-3}–0.14	kg·m^{-3}
c_{T}^{c}	$1.5 \times 10^{-3} - 8 \times 10^{-3}$	kg·m^{-3}
$D_{\mathrm{A}w}$	2.409×10^{-6}	m^2·h^{-1}
$D_{\mathrm{A}b}$	1.205×10^{-6}	m^2·h^{-1}
$D_{\mathrm{T}w}$	8.280×10^{-6}	m^2·h^{-1}
$D_{\mathrm{T}b}$	4.140×10^{-6}	m^2·h^{-1}
L_{b0}	4	µm
Δx, Δy	4	µm
Δt_g	1	h
$\rho_b^{\max}$	70	kg·m^{-3}

Biofilms presented in Fig. 3a and 3b grew under conditions of significantly different concentrations of the limiting substrate in the bulk liquid. Results were obtained for two values of G group, 1.3 and 7, respectively.

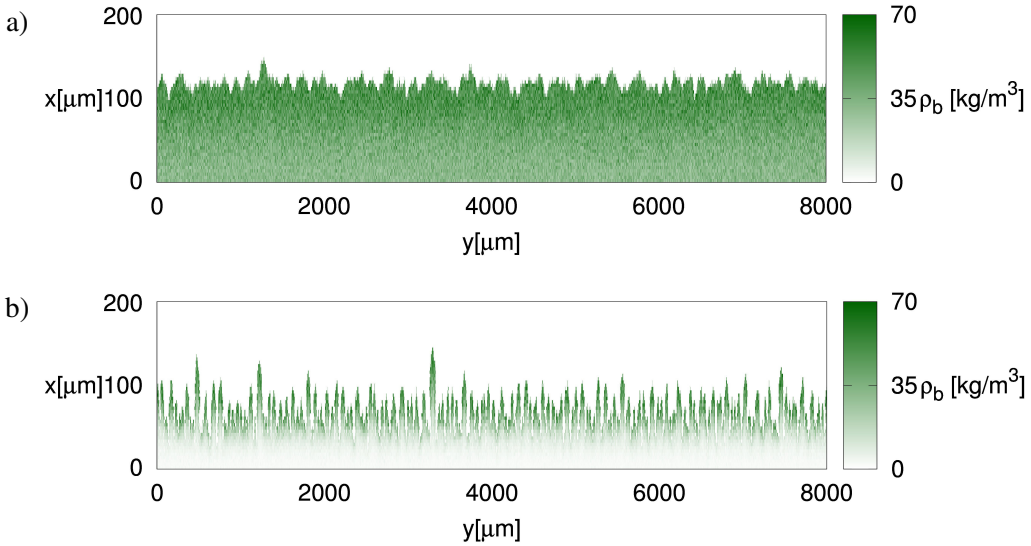

Fig. 3. Two-dimensional distributions of biofilm density for *Nitrosomonas europaea* bacteria; a) $G = 1.3$; b) $G = 7$

It can be seen from Fig. 3 that transport limitation results in significant irregularity of biofilm. It arises from the fact that voids formed between colonies cannot be filled due to insufficient amount of substrate for the growth of biomass. In Fig. 3b biofilm density at its bottom is very low. This is due to the form of the kinetic model, according to which at low limiting substrate concentrations the rate of biomass growth r_B can be negative, what should be interpreted as death of microorganisms. When the concentration of the substrate is equal to zero, the microorganisms die at a maximum rate equal:

$$r_o^b(\rho_b) = w_{\mathrm{BT}} m_{\mathrm{T}} \rho_b = k_o \rho_b \tag{9}$$

Although Fig. 3a and 3b show the biofilms of the same thickness, the time of their growth is significantly different due to different concentrations of the limiting substrate in the liquid phase. Biofilm shown in

Fig. 3a due to relatively large value c_A^c has reached a thickness of 150 μm after 192 h, and that shown in Fig. 3b after 890 h. After this time most of microorganisms in the bottom of the biofilm, because of lack of the substrate for growth, die and reduce the biomass density. Increase in biofilm porosity with decrease in substrate concentration is consistent with results of research by Wijeyekoon et al. (2004) conducted on biofilms of ammonia oxidizing bacteria. From the other side, Tijhuis et al. (1994) shown that in biofilm air-lift reactor an increased substrate loading resulted in a more porous biofilm. Contradictory results of experimental studies are probably due to hydrodynamic conditions in bioreactors used in both works. Wijeyekoon et al. (2004) used a tubular bioreactor, in which the character of the liquid flow was laminar. In turn, the air-lift bioreactor is characterized by intensive mixing of the reaction environment, which favors minimizing external mass transfer resistances to the biofilm. According to de Beer and Stoodley (1995) at high flow velocity the shape of the upper limit of the mass boundary layer follows the biofilm surface, whereas at lower flow velocity it becomes parallel with the substratum surface. In the mathematical model used in this study it is assumed that the upper limit of the mass boundary layer is parallel to substratum, therefore corresponding to low flow velocity, as in the case of Wijeyekoon research.

A numerical experiment was carried out, aimed at determining the influence of the group G on the structure of the biofilm of heterotrophic *Pseudomonas aeruginosa* bacteria in the process of degradation of glucose. These bacteria are often used in experimental studies on biofilms (Peyton, 1996; Stewart et al., 1993). In the calculations, single-substrate Monod kinetics was used:

$$r_A^b\left(c_A^b, \rho_b\right) = \frac{k}{w_{BA}} \cdot \frac{k c_A^b}{K_A + c_A^b} \rho_b \tag{10a}$$

$$r_B^b\left(c_A^b, \rho_b\right) = \frac{k c_A^b}{K_A + c_A^b} \rho_b \tag{10b}$$

$$r_o^b(\rho_b) = k_o \rho_b \tag{10c}$$

Kinetic parameters determined by Bakke et al. (1984) were accepted. According to this kinetic model limiting substrate is glucose. In the cited work and in other publications on kinetic studies of this microbiological process (Beyenal et al., 2003; Robinson et al., 1984), death rate coefficient of microorganisms was not determined. The presented work initially did not take into account death of microorganisms and the influence of this phenomenon on the biofilm structure will be discussed later in the article. Two-dimensional biofilm density distributions obtained without taking into account the death of microorganisms are shown in Fig. 4. Similarly as in Fig. 3, biofilms have a thickness of 150 μm. The results show that for the given microbiological process the biofilm is compact, nearly flat, for both G group, in opposite to the above-described oxidation of ammonium by *Nitrosomonas europaea* bacteria.

Figure 5 shows two-dimensional density distributions of the biofilm for the same process as in Fig. 4, but for a thickness of 300 μm and for lower concentration of limiting substrate in the liquid, i.e. for $G = 40$ (Fig. 5a), $G = 200$ (Fig. 5b) and $G = 400$ (Fig. 5c). It arises from Fig. 5 that the increase in value of the group G due to higher diffusional resistance results in the formation of biofilm of an increasingly irregular structure, however these changes are not as visible as in Fig. 3. It can be summarized that the value of G group, defined by Eq. (7), for which the biofilm structure becomes irregular will be different for different growth kinetics. Difference in those critical G values is probably caused by that the death rate coefficient and saturation constant are not taken into account in the G group, despite those parameters also influence the process rate.

Figure 6 presents two-dimensional density distributions of the biofilm for glucose biodegradation, but with taking into account the death of microorganisms. Values of death rate coefficient were accepted according to Anguige and co-authors (2005) equal to $k_o = 10^{-4}$ h^{-1} (Fig. 6a), value ten-fold higher, i.e. $k_o = 10^{-3}$ h^{-1} (Fig. 6b) and $k_o = 5.6 \cdot 10^{-3}$ h^{-1} (Fig. 6c). The last value of death rate coefficient has been determined for

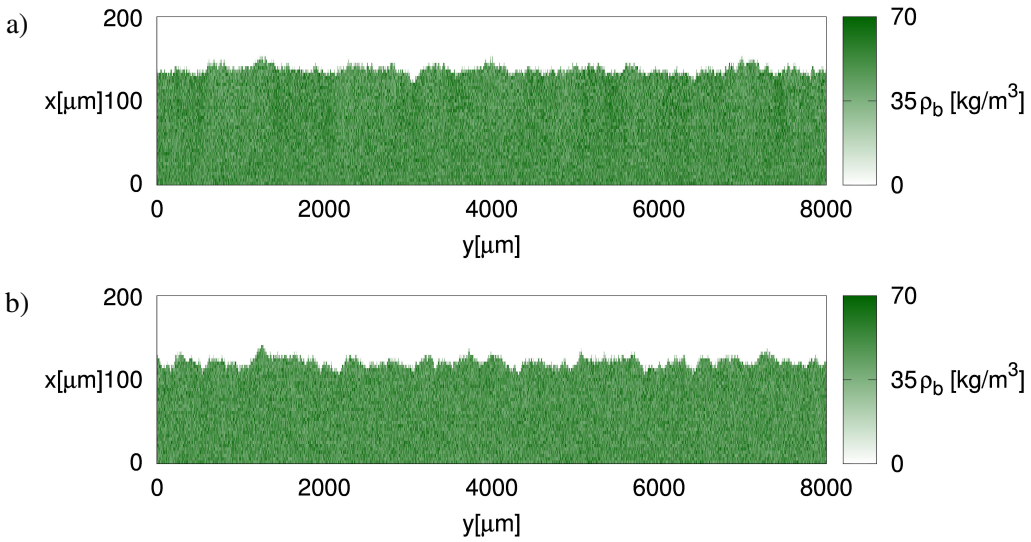

Fig. 4. Two-dimensional distributions of biofilm density for *Pseudomonas aeruginosa*; a) G = 2 (t = 192 h); b) G = 10 (t = 890 h)

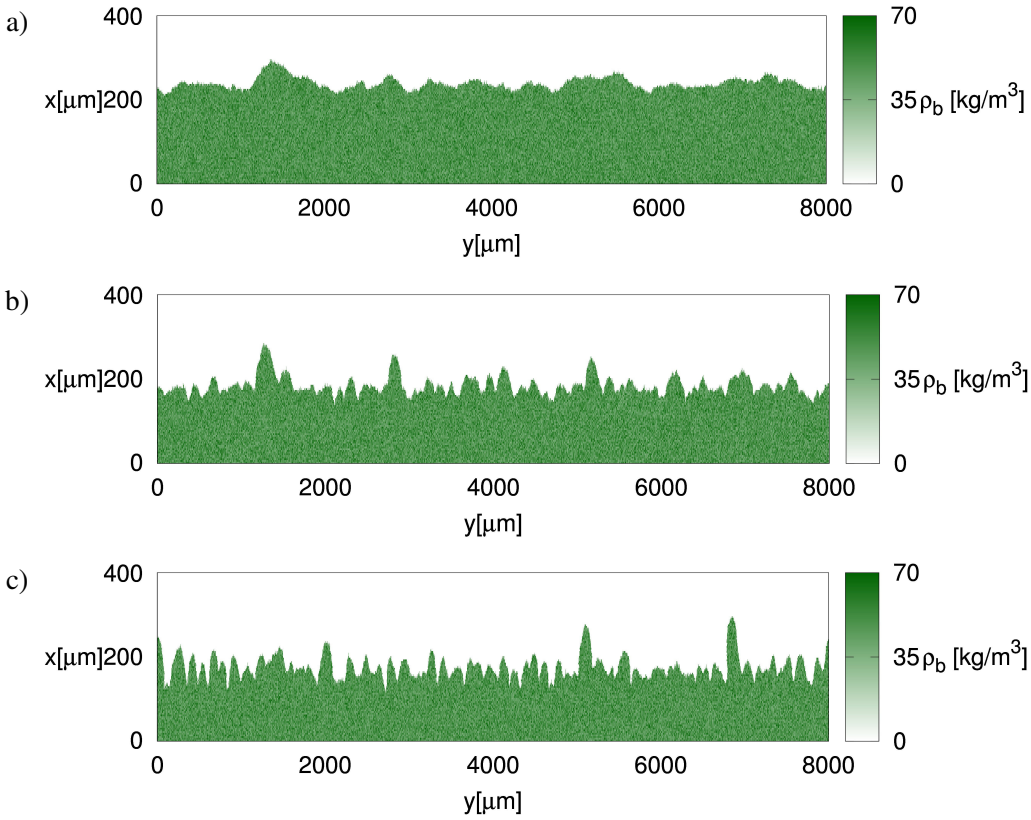

Fig. 5. Two-dimensional distributions of biofilm density for *Pseudomonas aeruginosa*; a) G = 40 (t = 40 h); b) G = 200 (t = 125 h); c) G = 400 (= 245 h)

Pseudomonas putida bacteria (Kumar et al., 2005). The value of G is the same as in Fig. 5b. The structures of biofilms in Fig. 5b and 6a are similar. It can be seen in Fig. 6b that density at the biofilm bottom reaches slightly lower values than maximum, while Fig. 6c indicates a strong effect of death of microorganisms on biomass density distribution.

For the adopted values of kinetic parameters of the Wijffels model (Eqs. (8)), the value of death rate coefficient is $k_o = w_{\mathrm{BT}} \cdot m_{\mathrm{T}} = 0.00486\ \mathrm{h}^{-1}$, so for the oxidation of ammonium the ratio of the death

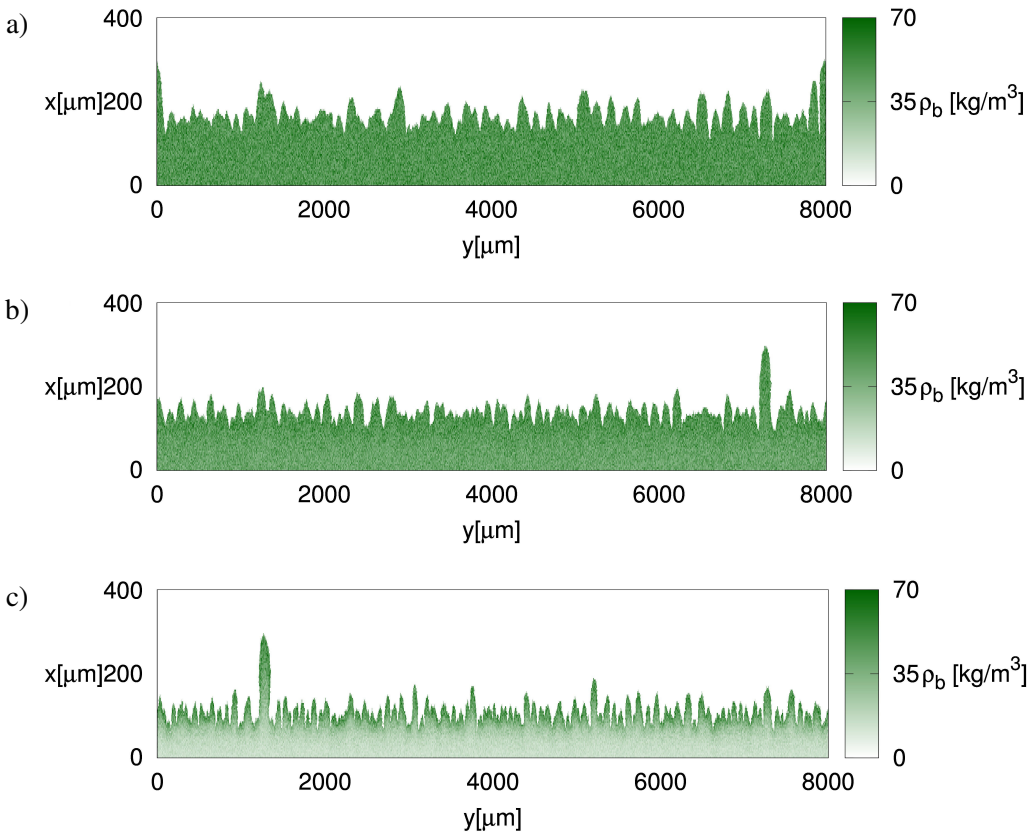

Fig. 6. Two-dimensional density distributions of *Pseudomonas aeruginosa* biofilm; a) $k_o = 1.0 \cdot 10^{-4}$ h^{-1}; b) $k_o = 1.0 \cdot 10^{-3}$ h^{-1}; c) $k_o = 5.6 \cdot 10^{-3}$ h^{-1}

rate coefficient to the maximum specific growth rate of microorganisms is $k_o/k = 0.089$, while for the single-substrate glucose biodegradation following Monod model (Eqs. (10)) for the highest of the adopted values of death rate coefficient is $k_o/k = 0.014$. Microbiological process following Eqs. (8) can be defined as a slowly growing bacteria with high death rate, while following Eqs. (10) as a rapidly growing bacteria with low death rate.

For a better illustration of the influence of death rate coefficient on biofilm structure, Fig. 7 shows one-dimensional distributions of biofilm density (Fig. 7a) and its porosity (Fig. 7b). These relationships are determined by averaging the density and porosity of the biofilm along the coordinate y in the cells of cellular automata. Figure 7a shows that increasing the death rate coefficient causes a qualitative change in the distribution of biofilm density – for sufficiently large k_o values a maximum of $\rho_b(z)$ is observed.

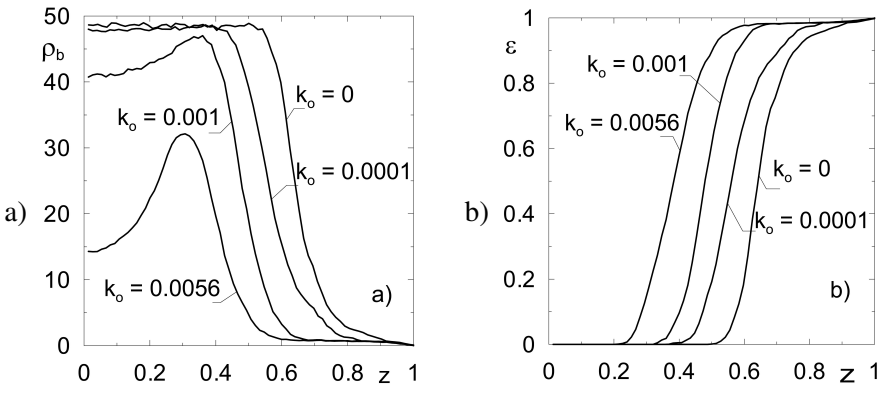

Fig. 7. One-dimensional distributions of density (Fig. 7a – left) and porosity (Fig. 7b – right) of *Pseudomonas aeruginosa* biofilm for different values of death rate coefficient

Figure 7b shows that with increase in death rate coefficient biofilm porosity increases, and the thickness of the compact layer of the biofilm biomass at the bottom decreases. One-dimensional distributions of density are usually determined empirically. They are useful for modeling bioreactors with biofilm by continuous models using, i.e. based on differential calculus.

4. CONCLUSIONS

In the study a mathematical model based on the theory of cellular automata was used to model growth of biofilms, in which the microbiological process follows two different unstructured single-substrate kinetic models. The mathematical model of biofilm growth takes into account substrate diffusion, its utilization, growth and displacement of microorganisms and death of microorganisms. It was shown that biofilms of both considered microbiological processes can form flat or heterogeneous structure depending on growth conditions. For the oxidation of ammonium, biofilm structure is highly irregular for $G > 7$ while for glucose biodegradation, biofilm becomes irregular for $G > 400$. Qualitative comparison of biofilm structures was based on two-dimensional density distribution of biomass. Based on those distributions the one-dimensional density and porosity distributions were obtained which allow for quantitative comparison of the biofilm structure.

It was shown that the death rate of microorganisms exerts strong influence on the density and porosity of the biofilm and therefore will affect the rate of transport of reactants and rate of the microbiological process. Therefore, this phenomenon should be taken into account during the modeling and simulation of biofilm growth and bioreactors with biofilm.

SYMBOLS

c_A, c_T	mass concentration of the carbonaceous substrate and oxygen, respectively, kg·m^{-3}
D_i	diffusion coefficient of i component, m^2·h^{-1}
G	dimensionless group, –
k	maximum specific growth rate, h^{-1}
K_i	saturation constant for substrate i, kg·m^{-3}
k_o	death rate coefficient, h^{-1}
L_b	biofilm thickness, μm
m_i	maintenance coefficient for substrate i, kg i·(kg B·h)$^{-1}$
N	number of iterations, –
r_A, r_B, r_T	uptake rate of the carbonaceous substrate, growth rate of bacteria and uptake rate of oxygen, respectively, kg i·m^{-3}·h^{-1}
r_o	death rate of bacteria, kg·m^{-3}·h^{-1}
t	time, h
w_{BA}, w_{BT}	yield coefficients, kg B·(kg i)$^{-1}$
x, y	space coordinates in the biofilm, μm
z	dimensionless coordinate of the biofilm thickness, –
Δt	time step for diffusion and utilization of substrates rules, h
Δt_g	time step for growth and death rule, h
Δx, Δy	grid cell size, m
ε	biofilm porosity, –
μ	cell state, –
ρ_b	biofilm density, kg·m^{-3}

ρ_b^{max} maximum biofilm density, kg·m^{-3}

Superscripts

c liquid (continuous) phase
b biofilm

Subscripts

A carbonaceous substrate (glucose)
b biofilm
T oxygen
w water

REFERENCES

Anguige K., King J.R., Ward J.P., 2005. Modelling antibiotic- and anti-quorum sensing treatment of a spatially-structured Pseudomonas aeruginosa population. *J. Math. Biol.*, 51, 557–594. DOI: 10.1007/s00285-005-0316-8.

Bakke R., Trulear M.G., Robinson J.A., Characklis W.G., 1984. Activity of *Pseudomonas aeruginosa* in biofilms: Steady state. *Biotechnol. Bioeng.*, 26, 1418–1424. DOI: 10.1002/bit.260261204.

Beyenal H., Chen S.N., Lewandowski Z., 2003. The double substrate growth kinetics of *Pseudomonas aeruginosa*. *Enzyme Microb. Technol.*, 32, 92–98. DOI: 10.1016/S0141-0229(02)00246-6.

de Beer D., Stoodley P., 1995. Relation between the structure of an aerobic biofilm and transport phenomena. *Water Sci. Technol.*, 32, 11–18. DOI: doi:10.1016/0273-1223(96)00002-9.

Duddu R., Chopp D.L., Moran B., 2009. A two-dimensional continuum model of biofilm growth incorporating fluid flow and shear stress based detachment. *Biotechnol. Bioeng.*, 103, 92–104. DOI: 10.1002/bit.22233.

Flint S.H., Brooks J.D., Bremer P.J., 2000. Properties of the stainless steel substrate, influencing the adhesion of thermo-resistant streptococci. *J. Food Eng.*, 43, 235–242. DOI: 10.1016/S0260-8774(99)00157-0.

Kreft J., Picioreanu C., Wimpenny J.W.T., van Loosdrecht M.C.M., 2001. Individual-based modelling of biofilms. *Microbiol.*, 147, 2897–2912. DOI: 10.1099/00221287-147-11-2897.

Kułakowski K., 2000. *Automaty komórkowe*. OEN AGH, Kraków.

Kumar A., Kumar S., Kumar S., 2005. Biodegradation kinetics of phenol and catechol using *Pseudomonas putida* MTCC 1194. *Biochem. Eng. J.*, 22, 151–159. DOI: 10.1016/j.bej.2004.09.006.

Peyton B.M., 1996. Effects of shear stress and substrate loading rate on *Pseudomonas aeruginosa* biofilm thickness and density. *Water Res.*, 30, 29–36. DOI: 10.1016/0043-1354(95)00110-7.

Picioreanu C., van Loosdrecht M.C.M., Heijnen J.J., 1998a. A new combined differential-discrete cellular automaton approach for biofilm modeling: application for growth in gel beads. *Biotechnol. Bioeng.*, 57, 718–731. DOI: 10.1002/(SICI)1097-0290(19980320)57:6<718::AID-BIT9>3.0.CO;2-O.

Picioreanu C., van Loosdrecht M.C.M., Heijnen J.J., 1998b. Mathematical modeling of biofilm structure with a hybrid differential-discrete cellular automaton approach. *Biotechnol. Bioeng.*, 58, 101–116. DOI: 10.1002/(sici)1097-0290(19980405)58:1<101::aid-bit11>3.0.co;2-m.

Robinson J.A., Trulear M.G., Characklis W.G., 1984. Cellular reporoduction and extracellular polymer formation by *Pseudomonas aeruginosa* in continuous culture. *Biotechnol. Bioeng.*, 26, 1409–1417. DOI: 10.1002/bit.260261203.

Skoneczny S., 2015. Cellular automata-based modelling and simulation of biofilm structure on multi-core computers. *Water Sci. Technol.*, 72, 2071–2081. DOI: 10.2166/wst.2015.426.

Skoneczny S., 2017. Cellular automata as an effective tool for modelling of biofilm morphology. *Environ. Prot. Eng.*, 43, 4, 177–190. DOI: 10.5277/epe170414.

Stewart P.S., Peyton B.M., Drury W.J., Murga R., 1993. Quantitative observations of heterogeneities in Pseudomonas aeruginosa biofilms. *Appl. Environ. Microbiol.*, 59, 327–329.

Tijhuis L., Van Loosdrecht M.C.M., Heijnen J.J, 1994. Formation and growth of heterotrophic aerobic biofilms on small suspended particles in airlift reactors. *Biotechnol. Bioeng.*, 44, 595–608. DOI: 10.1002/bit.260440506.

Wijeyekoon S., Mino T., Satoh H., Matsuo T., 2004. Effects of substrate loading rate on biofilm structure. *Water Res.*, 38, 2479–2488. DOI: 10.1016/j.watres.2004.03.005.

Wijffels R.H., Schepers A.W., Smit M., de Gooijer C.D., Tramper J., 1994. Effect of initial biomass concentration on the growth of immobilized *Nitrosomonas europaea*. *Appl. Microbiol. Biotechnol.*, 42, 153–157. DOI: 10.1007/BF00170239.

APPENDIX

BIOMASS SPREADING ALGORITHM

1. Assign the coordinates of the biomass grid cell in which the maximum biofilm density has been exceeded to indexes $[k, l]$. Change the cell state to $0.5 \cdot \mu$. Create an auxiliary variable ν and set its value to $\nu = 0.5 \cdot \mu$.
2. Check if there is at least one cell with state $\mu = 0$ in the neighborhood of the cell with indexes $[k, l]$. If so, choose one cell from these cells randomly. Change the state of this cell from $\mu = 0$ to $\mu = \nu$. Finish the algorithm.
3. If in the neighborhood of the biomass grid cell with indexes $[k, l]$ there is no cell with the state $\mu = 0$, then choose one of these cells randomly. Set the variable ν to the state of the chosen cell, i.e. $\nu = \mu$, and change the state of the chosen cell to the value of the variable ν before this assignment. Change the indexes k and l to the coordinates of the chosen cell. Go to step 2.

The operation of the algorithm is illustrated in Fig. A1. In the presented example, the maximum biomass density was exceeded in the cell marked with dark grey. It is surrounded only by cells indicating the biomass presence, which are marked with light grey. One of them is chosen randomly. Its state is changed from μ_2 to $0.5\mu_1$ and successive cell is chosen randomly, as there is no free cell in the neighborhood. The cell state is changed from μ_3 to μ_2. As there are free cells in the neighborhood (white color) one of those free cells is chosen randomly and its state is set to μ_3.

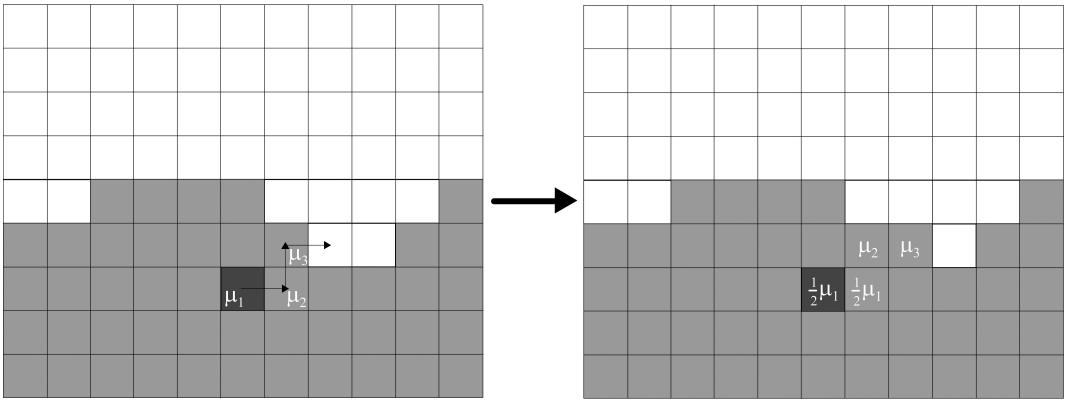

Fig. A1. Illustration of the algorithm of biomass spreading; left image shows the biomass grid before the execution of the algorithm, while right one after its execution; white color – water, grey color – biofilm

Received 23 October 2016
Received in revised form 22 February 2019
Accepted 25 February 2019